A New Reflectivity Index for the Retrieval of Surface Soil Moisture From Radar Data

Mehrez Zribi, Myriam Foucras, Nicolas Baghdadi, Jerome Demarty, and Sekhar Muddu

***Abstract*—A new approach based on the change detection technique is proposed for the estimation of surface soil moisture (SSM) from a time series of radar measurements. A new index of reflectivity (IR) is defined that uses radar signals and Fresnel coefficients. This index is equal to 0 in the case of the smallest value of the Fresnel coefficient, corresponding to the driest conditions and the weakest radar signal, and is equal to 1 for the highest value of the Fresnel coefficient, corresponding to the wettest soil conditions and the strongest radar signal. The integrated equation model is used to simulate the behavior of radar signals as a function of soil moisture and roughness. This approach validates the greater usefulness of the IR compared with that of the commonly used index of SSM (I_{SSM}), which assumes that the SSM varies linearly as a function of radar signal strength. The *IR*-based approach was tested using Sentinel-1 radar data recorded over three regions: Banizombou (Niger), Merguellil (Tunisia), and Occitania (France). The *IR* approach was found to perform better for the estimation of SSM than the I_{SSM} approach based on comparisons with ground measurements over bare soils.**

***Index Terms*—Change detection, index of reflectivity (IR), index of surface soil moisture (ISSM), Sentinel-1, surface soil moisture (SSM), radar.**

I. Introduction

SOIL moisture is an essential parameter for analyzing interactions between the Earth's surface and the atmosphere as well as the manner in which precipitation is ultimately allocated among the three main processes of runoff, infiltration, and evapotranspiration [1]–[3]. In this context, remote sensing has demonstrated its considerable potential for monitoring the water content of soil surfaces [4], [5]. Several different approaches have been used for this purpose, based primarily on the interpretation of passive and active microwave observations [6]–[15].

The first methods to be proposed were based on the use of data from the Soil Moisture and Ocean Salinity [7] and Soil Moisture Active and Passive [9] missions and produced surface soil moisture (SSM) estimations at relatively low spatial resolutions of approximately 10–50 km. So-called active radar missions involve the use of synthetic aperture radar (SAR) data and low-resolution scatterometers. Methods based on the use of SAR data are generally applied at the scale of agricultural fields [16]–[26] or at scales close to 1 km resolution [27]–[29]; in recent years, they have become more consistent and operational thanks to the arrival of the Sentinel-1 Copernicus constellation [28], [29]. In this context, there are three main approaches to the inversion of radar signals: one is based on direct inversion of physical models [30]–[32], a second is based on statistical techniques such as neural networks [33]–[36], and the other is based on the use of change detection algorithms [37]–[40].

The change detection approach was first applied at a low spatial resolution with data provided by the European Remote Sensing Satellite and the Advanced SCATterometer instrument on the METeorological OPerational satellite platform of the European Space Agency [37]. This approach was used to develop an operational product at resolutions of 12.5 and 25 km for water content monitoring at global scales and for operational applications. A moisture index between 0 and 1 was proposed, with 0 corresponding to the weakest radar signal and thus to the driest soil conditions and 1 corresponding to the strongest radar signal and thus to the wettest soil conditions, with the model assuming a linear relationship between radar signal strength and soil moisture. This approach has been generalized to other applications at medium and high spatial resolutions. Bauer-Marschallinger *et al.* [28] thus developed soil moisture products at a 1-km spatial resolution using Sentinel-1 data, and these products are now used operationally for the European continent. The results illustrate the strong potential of this method, despite limitations in certain areas resulting from inaccurate modeling of the influence of vegetation on the backscattered radar signals [41]. Gao *et al.* [39] also proposed an application based on the change detection technique for the study of soil moisture at a scale equivalent to the size of agricultural plots. These authors took the influence of vegetation cover into account and used optical images from the Sentinel-2 satellite to assess temporal variations in surface-scattered Sentinel-1 radar signals. Tomer *et al.* [40] proposed an approach based on cumulative density function matching, which is more sophisticated than the simple hypothesis of linearity between soil moisture and RADARSAT-2 radar signal strength. For all applications at high spatial resolutions, an accuracy generally better than 0.06 m^3/m^3 is achieved when this moisture index is converted to volumetric moisture. In

Manuscript received August 10, 2020; revised September 28, 2020; accepted October 10, 2020. Date of publication October 22, 2020; date of current version January 6, 2021. This work was supported in part by the French National Centre for Space Studies (TAPAS TOSCA program) and in part by the European Space Agency (Irrigation+ program). *(Corresponding author: Mehrez Zribi.)*

Mehrez Zribi and Myriam Foucras are with the Centre d'Etudes Spatiales de la Biosphère, 31401 Toulouse, France (e-mail: mehrez.zribi@ird.fr; myriam.foucras@cesbio.cnes.fr).

Nicolas Baghdadi is with the INRAE, TETIS, University of Montpellier, 34093 Montpellier, France (e-mail: nicolas.baghdadi@teledetection.fr).

Jerome Demarty is with Hydro Sciences Montpellier (HSM), University of Montpellier, IRD, CNRS, 34090 Montpellier, France (e-mail: jerome.demarty@ird.fr).

Sekhar Muddu is with the Indian Institute of Science, Bangalore 560012, India (e-mail: sekhar.muddu@gmail.com).

Digital Object Identifier 10.1109/JSTARS.2020.3033132

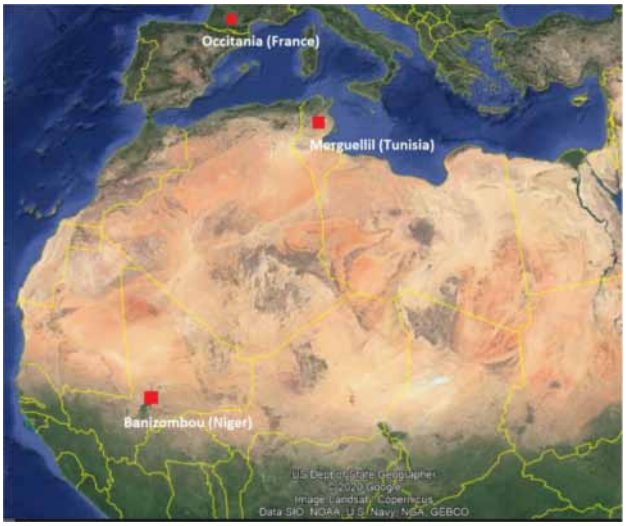

Fig. 1. Studied sites [Banizombou (Niger), Merguellil (Tunisia), Occitania (France)].

conclusion, the main advantage of change detection approach is the simplicity of the proposed algorithms, the limitation of the number of input parameters, with high precision of the estimates. On this basis, it is suitable for an operational application.

In parallel with the aforementioned methods used for the inversion of radar signals, theoretical simulations and various experimental studies [42]–[46] have long shown that the relationship between radar signal strength and SSM is nonlinear, as clearly illustrated by the radar signal saturation at high soil moisture levels. Thus, despite the generally accurate estimations achieved with the change detection approach, the assumption of linearity between radar signals and SSM can lead to inaccurate soil water content estimations under extreme conditions, as has already been observed in areas affected by high moisture levels [47].

The purpose of this article is to propose an improved approach that is based on the change detection technique but takes into account the observed nonlinearity of variations in radar signal strength as a function of soil moisture.

Section II presents the study sites and data described in this article. Section III describes the proposed methodology and introduces our new index of reflectivity (IR). Section IV presents the results and discusses the application of the proposed approach to three study sites based on Sentinel-1 time series data. Our conclusions are presented in Section V.

II. Study Sites and Databases

A. Study Sites

In the present study, three sites were investigated. These sites, located in West Africa (Niger), North Africa (Tunisia), and Occitania (France) (Fig. 1), were equipped with ground stations.

1) Niger Site: The ground measurements were carried out in southwestern Niger, near Banizombou, between the Niger River and the fossil valley of Dallo Bosso. This is a portion of a one square degree area (12–13°N, 2–3°E), defined in 1992 for the purposes of the international Hapex–Sahel survey and the African Monsoon Multidisciplinary Analysis–Coupling the Tropical Atmosphere and the Hydrological Cycle observatory [48], [49]. The Sahelian climate in this region is semiarid, with an average annual rainfall ranging between 300 and 750 mm, and is characterized by a rainy season from June to September. The landscape is mainly flat and is dominated by dissected plateaus with slopes of less than 6%. The plateaus have lateritic soils and are partly covered with tiger bushes. These plateaus are surrounded mostly by terrain with strong transitional features and steep inclines that can have slopes of up to 35%. Vegetation in the valleys is dominated by cultivated (mainly millet) and fallow fields. Over the studied site, a network of two continuous Thetaprobe stations (Delta T Devices) installed in locations with bare soil provided moisture measurements every 1 h, near Banizombou (∼12°43′N; 2°30′E). At each station, all *in situ* measurements were made at depths of 5 cm and were calibrated using gravimetric measurements. The data for this site can be obtained from the International Soil Moisture Network.[1]

2) Merguellil Site: The Merguellil site is located in central Tunisia (9°54′E; 35°35′N). It is characterized by a semiarid climate with highly variable rainfall patterns, very dry summer seasons, and wet winters. The average annual rainfall is approximately 300 mm/year [17]. The studied site is in an agricultural region where the dominant croplands are mainly olive groves and cereal fields; the croplands have large irrigated perimeters that mobilize large quantities of water for agricultural production. Over the studied site, a network of seven continuous Thetaprobe stations installed in locations with bare soil provided moisture measurements every 3 h. At each station, the measurements were made at depths of 5 cm. All soil moisture measurements were calibrated using gravimetric measurements. Four stations covering the period of Sentinel-1 measurements are considered in this article (Barrage (∼35°35′N; 9°45′E), Barrouta (∼35°36′N; 10°04′E), Bouhajla (∼35°21′N; 10°12′E) and INGC (∼35°37′N; 9°56′E)). The data for this site can be obtained from http://osr-cesbio.ups-tlse.fr/.

3) Occitania Sites (France): The Occitania region was studied at several different sites close to the cities of Toulouse and Montpellier. The *in situ* SSM measurements were provided by the soil moisture observing system–meteorological automatic network integrated application (SMOSMANIA) observation system. SMOSMANIA is a long-term project that has been organized in an effort to acquire SSM profiles from automated weather stations in southwestern and southeastern France [50]. The stations were chosen in order to form a Mediterranean–Atlantic transect for studying the marked climatic gradient between the two coastlines. The SSM probes (ThetaProbes) were calibrated at all depths (5, 10, 20, 30 cm) by measuring the SSM from gravimetric soil samples collected during the installation. In this article, only the measurements at 5-cm depth were used. While this region mainly consists of croplands, the stations are generally located in grasslands. Two stations (at Mouthoumet (∼43°N; 2°31′E) and Narbonne (∼43°11N; 3°E) that are representative of climate and land cover types in the Occitania

[1][Online]. Available: https://ismn.geo.tuwien.ac.at/en/

region were analyzed in this article. Their mean temperatures ranged between 12.3 °C and 15.2 °C, and their mean annual precipitation ranged between 649 and 845 mm. Data for these stations can be obtained from the International Soil Moisture Network.[2]

B. Sentinel-1 Data

Sentinel-1A and Sentinel-1B images were acquired between December 2015 and the end of 2019. These two satellites circle the Earth in the same orbital plane, 180° from each other. Their SAR instruments operate in the C-band (5.4 GHz) and the interferometric wide-swath mode and have a spatial resolution of 10 m. Each satellite has a revisit time of 12 days, which implies an overall revisit time in Europe equal to six days. The sensors provide dual-polarization imagery (copolarization (VV) and cross-polarization (VH)) at an incidence angle ranging between 31° and 43°. We used Level-1 ground range detection products that are derived from focused SAR signals that have been detected, multilooked and projected to ground range using an Earth ellipsoid model [51].

The image processing was executed using the Sentinel Application Platform toolbox. The first step in this process converts the signal to obtain the backscattering coefficient. A terrain correction is then applied to correct for geometric distortions using a digital elevation model (DEM**),** specifically, the DEM derived from the Shuttle Radar Topography Mission at 30-m spatial resolution. Finally, thermal noise removal and a Lee filter are applied to reduce speckle effects. In the present article, only VV polarization data were considered.

III. Methodology

A. Behavior of IEM Backscattering Simulations Over Bare Soil

To analyze the behavior of radar signals backscattered by soil surfaces, we used the integrated equation model (IEM), which is considered to be the model that is best suited to a wide range of soil roughness values. In this article, all simulations were considered in the VV polarization, which corresponds to the data provided by the Sentinel-1 mission. The IEM is expressed as [43]

$$\sigma_{VV} = \frac{k^2}{2}\, e^{-2k_z^2 s^2} \sum_{n=1}^{+\infty} s^{2n} |I_{vv}^n|^2 \frac{W^{(n)}\left(-2k_x,\ 0\right)}{n!} \qquad (1)$$

where σ_{vv} is the backscattering coefficient, θ is the radar incidence angle, k is the wavenumber, $k_z = k \times \cos(\theta)$, $k_x = k \times \sin\!\sin(\theta)$, and s is the root mean surface height. I_{vv}^n is a function of the radar incidence angle, the relative dielectric constant of the soil, εr, and the Fresnel reflection coefficient. $W^{(n)}(-2k_x,\ 0)$ is the Fourier transform of the nth power of the surface correlation function.

[2][Online]. Available: https://ismn.geo.tuwien.ac.at/en/

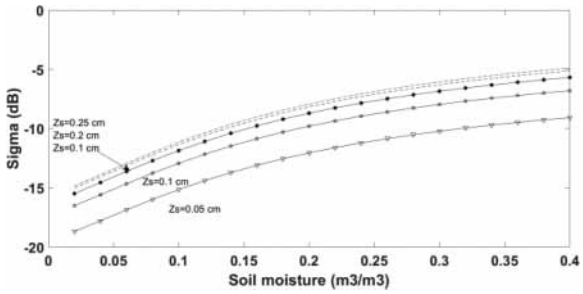

Fig. 2. Relationship between backscattering IEM simulations and soil moisture for different Z_s (roughness parameter) levels.

R_{vv} is the Fresnel coefficient for the *VV* polarization

$$R_{vv} = \frac{\cos(\theta) - \sqrt{\frac{1}{\varepsilon_r}\ \left(1 - \sin^2(\theta)\right)}}{\cos(\theta) + \sqrt{\frac{1}{\varepsilon_r}\ \left(1 - \sin^2(\theta)\right)}}\,. \qquad (2)$$

Fig. 2 provides a simulated view of IEM backscattering as a function of soil moisture and at different roughness levels. In this article, for the roughness description, we used the statistical parameter Z_s, which combines the effects of s and correlation length, as proposed by [52]. The effect of the autocorrelation function is very important in the simulation of soil scattering [53]. Only the exponential autocorrelation function, which is generally considered appropriate for natural surfaces, was used in the simulations illustrated in this article. However, we note that simulations using the Gaussian autocorrelation function produced the same conclusions. For these simulations, the SSM was considered to range between 0.03 m^3/m^3 and 0.4 m^3/m^3. In the IEM, the relative dielectric constant is computed from soil moisture using the Hallikainen model [54]. An approximately logarithmic relationship was found between the simulated radar signal (in VV polarization) and the two surface parameters, SSM and roughness (Z_s). The signal became almost saturated at high SSM values. When the soil moisture ranged between 0.3 and 0.4 m^3/m^3, the resulting increase in radar signal was close to 1 dB, corresponding to a slope of approximately 10 $dB/m^3/m^3$. However, when the SSM ranged between 0.1 and 0.3 m^3/m^3, the slope of this function increased to approximately 25 $dB/m^3/m^3$. The roughness effect was approximately the same for the entire moisture range, with an increase in the signal with roughness from $Z_s = 0.05$ cm to $Z_s = 0.25$ cm and a quasi-saturation of the simulated signal starting at $Z_s = 0.2$ cm. The simulation did not exceed $Z_s = 0.25$ cm to avoid IEM simulations out of its validity domain.

From these results and using the approximation of the small perturbation model [55], the radar signal σ_{VV} is considered to be the sum of a function that depends on roughness (g_{VV}) and another function that depends on the Fresnel coefficient (soil moisture) (f_{VV})

$$\sigma_{VV} = f_{VV}\ \left(log\left(R_{VV}\right)\right) + g_{VV}\left(Zs\right). \qquad (3)$$

Fig. 3 shows the *IEM*-simulated backscattering in the VV polarization (C-band) for the same range of values of SSM and Z_s as those used in Fig. 2. In this case, the simulated radar

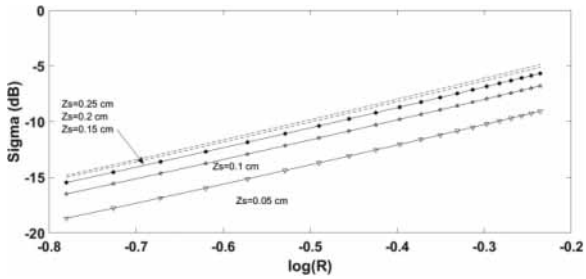

Fig. 3. Relationship between backscattering IEM simulations and log(R) for different Z_s (roughness parameter) levels.

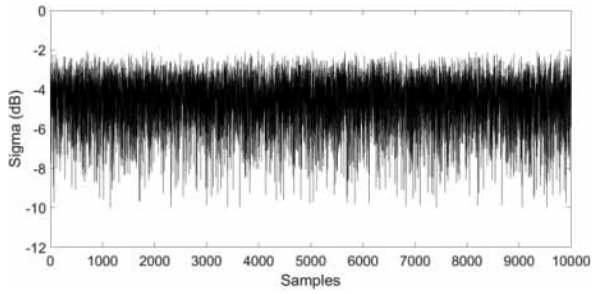

Fig. 4. IEM-simulated series for soil moisture ranging between 0 m^3/m^3 and 0.4 m^3/m^3, an rms height equal to 0.8 cm, and a correlation length equal to 6 cm.

signal strength is plotted as a function of the Fresnel coefficient ($\log(R_{vv})$) and for different Z_s values (0.05 cm, 0.1 cm, 0.15 cm, 0.2 cm, 0.25 cm). The radar signal is shown to have a nearly linear behavior as a function of ($\log(R_{vv})$) over the full range of roughness values, with a correlation coefficient (R^2) greater than 0.98. The function f_{VV} can thus be expressed as

$$f_{VV}\ (log\,(R_{VV})) = \alpha_{VV}\ \times\ log\,(R_{VV}) + \beta_{VV} \quad (4)$$

where α_{VV} is the slope of f_{VV} as a function of $\log(R_{VV})$ and β_{VV} is a constant parameter corresponding to the value of f_{VV} when R_{VV} is equal to 1.

B. Classical Soil Moisture Index, ISSM

The classical change detection SSM index $I_{\rm SSM}$ [34] is defined as

$$I_{\rm SSM} = \frac{\sigma_{VV} - \sigma_{VVmin}}{\sigma_{VV\max} - \sigma_{VV\min}} = \frac{SSM_t - SSM_{\min}}{SSM_{\max} - SSM_{\min}} \quad (5)$$

where SSM_t is the soil moisture content at time t; $\rm SSM_{min}$ and $\rm SSM_{max}$ are the minimum and maximum values of *in situ* soil moisture, respectively, measured at a depth of 5 cm; σ_{VV} is the radar signal at time *t*; and $\sigma_{VV\min}$ and $\sigma_{VV\max}$ are the minimum and maximum values of the radar signal time series, respectively.

To convert this index to volumetric soil moisture, we introduce

$$\rm SSM_t = I_{SSM}\ \times\ (SSM_{max} - SSM_{min}) +\ SSM_{min}. \quad (6)$$

C. New Reflectivity Index, IR

Based on the linear behavior described above, for the radar signal simulated as a function of the Fresnel coefficient (on a logarithmic scale), we propose a new reflectivity index. From (3) and (4), the index can be expressed as

$$\rm IR\ = \frac{\sigma_{VV} - \sigma_{VV\min}}{\sigma_{VV\max} - \sigma_{VV\min}} = \frac{\log|R_{VV}| - \log|R_{VV\min}|}{\log|R_{VV\max}| - \log|R_{VV\min}|} \quad (7)$$

where $R_{VV\min} = R(\rm SSM_{min})$, the minimum value of the Fresnel coefficient, and $R_{VV\max} = R(\rm SSM_{max})$, the maximum value of the Fresnel coefficient.

This IR is equal to zero for the weakest radar signal, corresponding to the lowest value of the Fresnel coefficient and thus to a minimum value of soil moisture. Similarly, this index is equal to 1 for the strongest radar signal, corresponding to the highest value of the Fresnel coefficient and thus to a maximum value of soil moisture.

A given value of the IR can be converted to volumetric soil moisture using the same approach as that proposed for the $I_{\rm SSM}$ using the minimum and maximum values of SSM for a given site

$$\log\left(R_{VV}\left(\rm SSM\right)\right) = \log\left(R_{VV\min}\left(SSM_{\min}\right)\right) + \rm IR \times \left(\log\left(R_{VV\max}\left(SSM_{\max}\right)\right) - \log\left(R_{VV\min}\left(SSM_{\min}\right)\right)\right). \quad (8)$$

From the theoretical relationship between $R_{VV}(\rm SSM_t)$ and the soil moisture, as defined in (2), the estimated value of $\log(R_{VV}(\rm SSM_t))$ can be inverted to retrieve the soil moisture, $\rm SSM_t$.

IV. Results and Discussion

A. Analysis of IR Potential Using an IEM Simulation Series With Constant Roughness

We produced a simulated series of IEM backscattering coefficients in the VV polarization at 5.3 GHz containing 10 000 samples with a Gaussian distribution that corresponded to a range of soil moisture between 0.03 and 0.4 m^3/m^3, a root mean square (rms) height equal to 0.8 cm, a correlation length equal to 6 cm, and an incidence angle equal to 40°. A noise signal respecting a Gaussian distribution and a standard deviation equal to 0.5 dB was added to the simulated radar signals to approximate real Sentinel-1 radar measurements [56]. Fig. 4 shows the resulting time series simulation.

Fig. 5(a) and (b) plots the estimated values of soil moisture as a function of the input values of soil moisture used for the simulations, retrieved using the $I_{\rm SSM}$ and the proposed IR, respectively. The IR was estimated from (7) using backscattering coefficients derived from the IEM simulations with additional Gaussian noise. The soil moisture was then calculated with (8). The minimum and maximum values of soil moisture used to compute $R_{VV\min}$ and $R_{VV\max}$ were derived from the input soil moisture series and applied to the IEM. The $I_{\rm SSM}$ was computed from (5) using backscattering coefficients derived from the IEM simulations with additional Gaussian noise. The SSM was then calculated with (6).

Fig. 5(a) and (b) shows that the IR-based approach leads to an improved estimation of the surface moisture, with a root mean

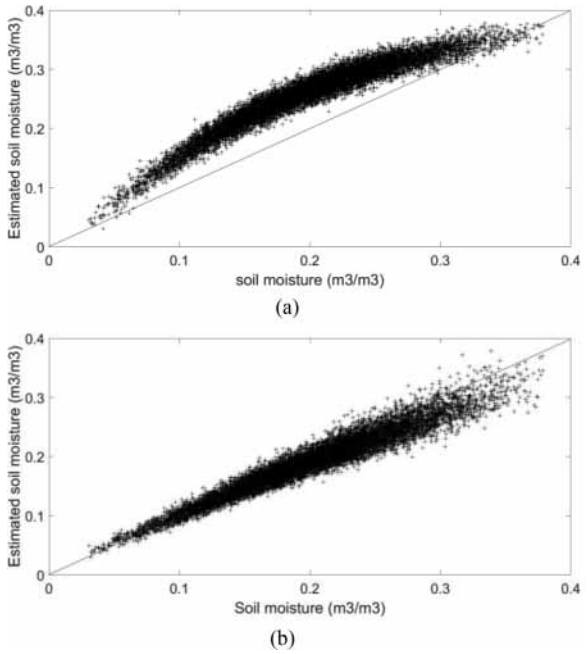

Fig. 5. Comparison between the input (actual) soil moisture used for the IEM simulations with constant roughness and the soil moisture estimations computed using two different indices. (a) I_{SSM}. (b) IR.

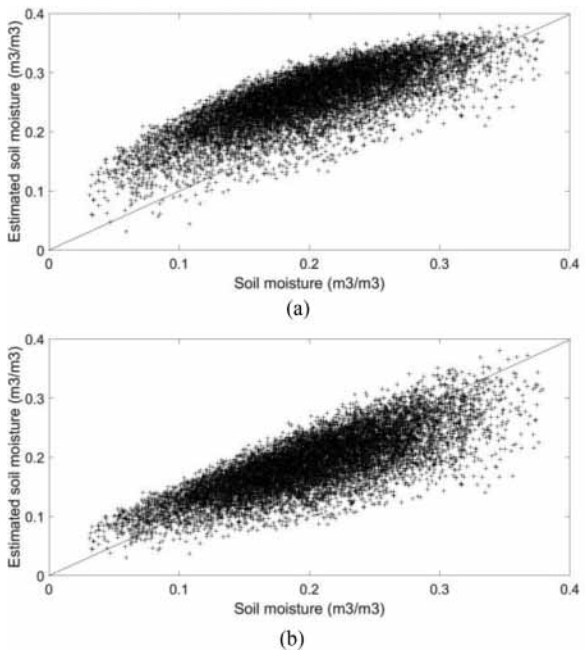

Fig. 6. Comparison between the input (actual) soil moisture used for the IEM simulations with variable roughness and the soil moisture estimations computed using two different indices. (a) I_{SSM}. (b) IR.

TABLE I
RMSE (m^3/m^3) BETWEEN ESTIMATIONS BASED ON IEM SIMULATIONS AND SOIL MOISTURE INPUTS FOR THE I_{SSM} AND IR ALGORITHMS FOR DIFFERENT SOIL MOISTURE RANGES AND ROUGHNESS CONDITIONS

Soil moisture range (m^3/m^3)	Constant roughness condition		Variable roughness condition	
	I_{SSM}	IR	I_{SSM}	IR
0-0.1	0.043	0.007	0.08	0.032
0.1-0.2	0.067	0.012	0.079	0.028
0.2-0.3	0.057	0.021	0.055	0.042
0.3-0.4	0.025	0.035	0.033	0.07

square error (RMSE) equal to 0.023 m^3/m^3, when compared to the values of soil moisture determined with estimations using I_{SSM}, for which the RMSE was equal to 0.055 m^3/m^3. With the latter index, the strongest bias was observed for average moisture values in the range of 0.1–0.2 m^3/m^3, since the model was initially calibrated with respect to the extreme values of soil moisture, i.e., values close to 0 and 0.4 m^3/m^3. In the IR-based approach, the errors in estimated soil moisture increased with increasing actual soil moisture. In particular, the accuracy of this method decreased for high moisture values due to the saturation of the radar signal and the resultant stronger effects of radar noise. RMSE values for all moisture ranges (0–0.1 m^3/m^3, 0.1–0.2 m^3/m^3, 0.2–0.3 m^3/m^3, 0.3–0.4 m^3/m^3) are provided in Table I. As noted above, the greatest difference between the two approaches was obtained at average values of soil moisture.

B. Analysis of IR Potential Using an IEM Simulation Series With Variable Roughness

As in Section IV-A, a series of IEM simulations of 10 000 samples with the same added noise is analyzed. In addition to the variation in soil moisture, we also include a roughness variation as input to the IEM simulations to evaluate its effect on IR potential. A Gaussian variation in the standard deviation of the heights, with a mean of 0.8 cm and a standard deviation of 0.2 cm, was used for the IEM simulations of the 10 000 samples. Fig. 6(a) and (b) plots the estimated values of soil moisture obtained using the I_{SSM} and the proposed IR, respectively, as functions of the soil moisture input values used for the simulations. For the proposed analysis, which used a variable roughness, the estimate based on IR showed higher precision, with an RMSE of 0.038 m^3/m^3, than the estimate based on I_{SSM} (RMSE of 0.068 m^3/m^3). Obviously, in both cases, the precision is much lower than that in simulations without variations in roughness. However, for the IR estimation, the RMSE remained below 0.05 m^3/m^3, which is generally taken as an acceptable threshold for the precision of soil moisture estimates. The maximum difference between the respective accuracies of IR and I_{SSM} remained in the range of 0.1–0.2 m^3/m^3, as shown in Table I. In the context of real data, roughness is rarely considered in proposed change detection algorithms. Using low-resolution data such as those from scatterometers [37] or working at average scales of approximately 1 km makes it possible to assume that the average roughness remains slightly variable. This assumption could decrease the precision of the estimates if there were important temporal changes in roughness.

C. Evaluation of the IR Across Three Study Sites

Following our validation of the proposed approach based on the IR, the method was applied to soil moisture data from eight ground stations located within the three study sites (Occitania, Merguellil, and Banizombou) described in Section II. Five of the selected ground stations (BZ1, BZ2, Bouhajla, Barrage, and

Barrouta) are characterized by a landscape with either bare soil or low-density vegetation cover, and three others (INGC, Mouthoumet, and Narbonne) are characterized by an agricultural landscape with important temporal dynamics in vegetation cover.

We identified a 1 km^2 zone centered around each moisture measurement station and derived an averaged radar signal (in the linear domain) for each Sentinel-1 acquisition for each zone. Only pixels with radar signal values between -20 and -5 dB were taken into account to avoid possible extremes from surfaces other than natural surfaces (such as water coverings or buildings) [28]. The choice of the 1 km^2 size was intended to limit the effects linked to roughness as much as possible and to enable the assumption of relatively stable average roughness. Indeed, in areas of limited size, the effect of roughness can be much greater and thus affect the proposed algorithm, as illustrated in Section IV-B. For each site, we considered data from one orbit with an approximately constant incidence angle. This approach notably reduced the number of images used by the change detection application but prevented errors resulting from empirical incidence angle normalization, which could change from one pixel to another and from one season to the next.

We then analyzed the Sentinel-1 data time series over a 4-year period. For each station, the I_{SSM} and IR values were converted to volumetric moisture as described in Section III and by using the ground moisture time series data. $\mathrm{SSM}_{\mathrm{min}}$ and $\mathrm{SSM}_{\mathrm{max}}$ represent the minimum and maximum values of *in situ* SSM at a depth of 5 cm at a given site (m^3/m^3) as defined by the 90% confidence interval of a Gaussian distribution [57]. By defining μ and σ as the mean and standard deviation of the ground-truth data over the study period used for this analysis, $\mathrm{SSM}_{\mathrm{min}}$ and $\mathrm{SSM}_{\mathrm{max}}$ can be computed as follows: $\mathrm{SSM}_{\mathrm{min}} = \mu - 1.65 \times \sigma$ and $\mathrm{SSM}_{\mathrm{max}} = \mu + 1.65 \times \sigma$, where 1.65 represents the 95% quantile of the standard normal distribution. It was preferred to use these quantities rather than the strict minimum and maximum values in order to eliminate outliers. In the general case of applications without ground measurements, it is possible to use soil texture maps to directly retrieve these hydrological properties through pedotransfer functions [58].

Figs. 7 and 8 compare the ground measurements with the soil moisture products estimated from Sentinel-1 data using the proposed IR and the classical I_{SSM} at two soil moisture stations. Strong agreement is observed between the ground measurements and the soil moisture estimated from the two considered indices. At the Barrouta site, RMSE and R are equal to 0.034 and 0.73 and to 0.04 and 0.74 for the *IR* and I_{SSM} approaches, respectively. At the INGC site, RMSE and R are equal to 0.06 m^3/m^3 and 0.6 and to 0.056 m^3/m^3 and 0.61 for the *IR* and I_{SSM} approaches, respectively.

However, differences in the rate at which the soil moisture decreases after rainfall events were noted. This is probably due to the effective penetration depth of the S1 radar, which is theoretically smaller than the value of 5 cm used for the ground-truth measurements [59]. In these cases, limited differences were observed between IR and I_{SSM}.

Table II summarizes the results obtained with the Sentinel-1 data products using I_{SSM} and IR. A strong correlation was

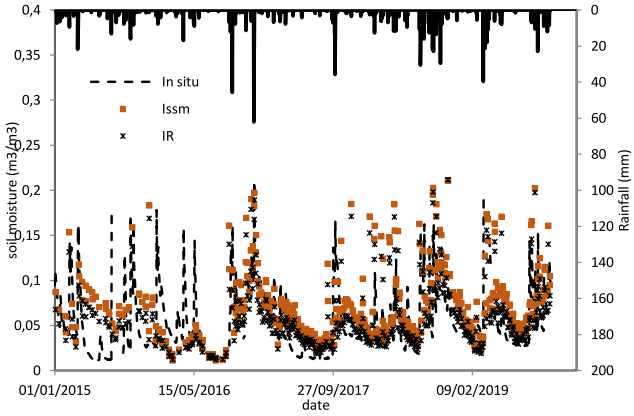

Fig. 7. Surface soil moisture estimations derived using the I_{SSM} and IR products compared with *in situ* measurements of soil moisture at the Barrouta site.

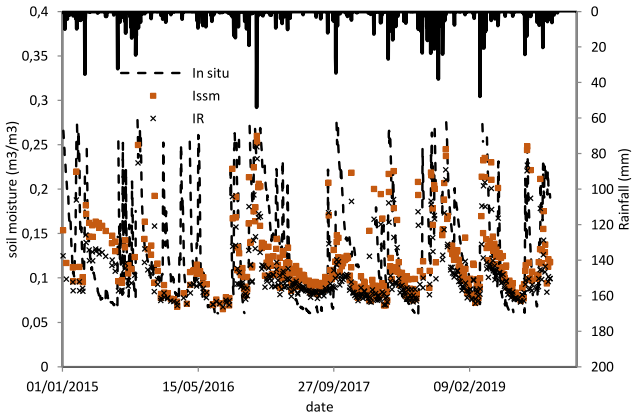

Fig. 8. Surface soil moisture estimations derived using the I_{SSM} and IR products compared with *in situ* measurements of soil moisture at the INGC site.

generally found between the ground measurements and the estimations for both indices, with an RMSE typically less than 0.06 m^3/m^3 for seven of the sites. At the five stations with bare soil or low vegetation cover, the IR index provided a limited improvement in accuracy for the soil moisture estimations, as indicated by its marginally lower RMSE values. For the other three stations, which had vegetation cover dynamics, IR shows slightly poorer accuracy than with I_{SSM}. The proposed index does not include any correction for the influence of vegetation.

Despite the overall results of the comparisons with the actual data, which showed high precision for both indices, the IR demonstrated its potential to provide accurate estimates of soil moisture. The correlation between ground measurements and remotely sensed soil moisture estimations is generally high. Some discrepancies can be attributed to the unpredictable conditions during precipitation events, which make it difficult to detect sporadic rainfall with radar acquisitions due to the 6- or 12-day repeat cycle of the Sentinel-1 constellation.

Compared to that in the analyses proposed in Sections IV-A and IV-B based on the IEM, the improvement provided by the IR seems lower in analyses with real

TABLE II
RMSE AND R FOR SURFACE SOIL MOISTURE (m^3/m^3) COMPUTED USING ISSM AND IR FOR ALL SITES

Site	I_{SSM}		IR	
	RMSE (m^3/m^3)	R	RMSE (m^3/m^3)	R
BZ1 (Niger)	0.019	0.81	0.018	0.82
BZ2 (Niger)	0.025	0.8	0.022	0.81
Bouhajla (Merguellil)	0.031	0.66	0.03	0.67
Barrage (Merguellil)	0.061	0.5	0.054	0.52
Barrouta (Merguellil)	0.04	0.74	0.034	0.73
INGC (Merguellil)	0.056	0.61	0.06	0.6
Mouthoumet (France)	0.048	0.42	0.05	0.41
Narbonne (France)	0.069	0.06	0.07	0.05

TABLE III
RMSE FOR SURFACE SOIL MOISTURE (m^3/m^3) COMPUTED USING ISSM AND IR FOR EACH SITE AND FOR EACH RANGE (0–0.1, 0.1–0.2, 0.2–0.3)

Site	0-0.1	0.1-0.2	0.2-0.3
BZ1	0.019/0.018	-	-
BZ2	0.025/0.022	0.017/0.019	-
Bouhajla	0.03/0.028	0.05/0.05	-
Barrage	0.058/0.04	0.067/0.08	-
Barrouta	0.04/0.032	0.04/0.047	
INGC	0.038/0.026	0.044/0.05	0.1/0.1
Mouthoumet	-	0.042/0.06	0.051/0.036
Narbonne	-	0.069/0.49	0.066/0.08

measurements. We retrieved approximately the same results with I_{SSM} as with IR. This difference may have several explanations. First, the size of the 4-year time series was likely too limited to obtain highly reliable statistics. High soil moisture radar data also tend to be noisier due to various effects, such as the temporal variations in soil roughness, which make it more difficult to reproduce the theoretical trends expected in the relationship between soil moisture and radar signal strength. At stations with temporal vegetation cover dynamics, errors may be more important, particularly during the wet season, when a strong vegetation effect that is not corrected for in the proposed algorithm occurs. At stations located in West Africa, the application context in semiarid areas could generate volume scattering on the driest dates [10] and high vertical soil moisture profile heterogeneity [59], which are also a source of errors in the application of the change detection technique.

The analysis of a relatively restricted database (4 years) does not allow us to observe the trends within each range of soil moisture (0–0.1 m^3/m^3, 0.1–0.2 m^3/m^3, and 0.2–0.3 m^3/m^3) with precision. Table III illustrates the RMSE observed for each site. The differences between the I_{SSM} and IR approaches are generally small.

V. CONCLUSION

A new inversion approach based on the change detection algorithm is proposed for the remotely sensed estimation of SSM. This approach is based on the near linearity of the relationship between backscattered radar signals and the logarithm of the Fresnel coefficient, which has been confirmed through the use of backscattering simulations based on the IEM. We thus introduce a new reflectivity index, IR, which ranges in value between 0 and 1. An index value of zero corresponds to the lowest value of the radar signal time series and thus to the driest conditions. An index value of 1 corresponds to the strongest radar signals and thus to the wettest conditions. IEM simulations of a series of radar signals with added noise, expressed as a function of soil moisture, confirmed the potential improvements that can be achieved with this index compared to the classical I_{SSM}, which assumes that the backscattered radar signals vary linearly as a function of soil moisture. In these simulations with constant roughness condition, the RMSE decreased from 0.055 to 0.023 m^3/m^3 when this new index was used. With introduction of roughness variation in IEM simulations, the RMSE decreased from 0.067 to 0.038 m^3/m^3 when IR was used.

The proposed algorithm was validated using Sentinel-1 data recorded over three study regions (Banizombou, Merguellil, and Occitania). Eight ground moisture stations (five with bare soil or low-density vegetation cover and three with agricultural landscapes showing temporal vegetation change) were used for this validation. For each station, when the IR was converted to volumetric moisture, it was found to be strongly consistent with ground measurements, with RMSEs of less than 0.06 m^3/m^3 for seven of the eight stations. When compared to the classical I_{SSM}, which assumes a linear relationship between soil moisture and radar signals, we observed almost the same precision with IR, with a slight improvements at stations with bare soils. This result is very encouraging, and we expect that even more robust results could be obtained with a longer time series. In the future, a more global analysis that considers the effect of vegetation cover will be performed.

ACKNOWLEDGMENT

The authors would also like to thank all of the AMMA-CATCH, SMOSMANIA, CESBIO and INAT teams for their strong collaboration and support for ground soil moisture measurements.

REFERENCES

[1] R. D. Koster *et al.*, "Regions of strong coupling between soil moisture and precipitation," *Science*, vol. 305, no. 5687, pp. 1138–1140, 2004.
[2] T. P. Anguela, M. Zribi, S. Hasenauer, F. Habets, and C. Loumagne, "Analysis of surface and root-zone soil moisture dynamics with ERS scatterometer and the hydrometeorological model SAFRAN-ISBA-MODCOU at grand morin watershed (France)," *Hydrol. Earth Syst. Sci.*, vol. 12, pp. 1415–1424, 2008.
[3] S. Manfreda, T. M. Scanlon, and K. K. Caylor, "On the importance of accurate depiction of infiltration processes on modelled soil moisture and vegetation water stress," *Ecohydrology*, vol. 3, pp. 155–165, 2009.
[4] F. T. Ulaby, G. Bradley, and M. C. Dobson, "Microwave backscatter dependence on surface roughness, soil moisture, and soil texture. II - Vegetation-covered soil," *IEEE Trans. Geosci. Remote Sens.*, vol. 17, no. 2, pp. 33–40, Apr. 1979.
[5] T. J. Jackson *et al.*, "Validation of advanced microwave scanning radiometer soil moisture products," *IEEE Trans. Geosci. Remote Sens.*, vol. 48, no. 12, pp. 4256–4272, Dec. 2010.

[6] L. Brocca, L. Ciabatta, T. Moramarco, F. Ponziani, N. Berni, and W. Wagner, "Use of satellite soil moisture products for the operational mitigation of landslides risk in central Italy," in *Satellite Soil Moisture Retrieval*. New York, NY, USA: Elsevier, 2016, pp. 231–247.

[7] Y. Kerr *et al.*, "The SMOS soil moisture retrieval algorithm," *IEEE Trans. Geosci. Remote Sens.*, vol. 50, no. 5, pp. 1384–1403, May 2012.

[8] S. Mecklenburg, J. Font, and R. Crapolicchio, "ESA's soil moisture and ocean salinity mission: Mission performance and operations," *IEEE Trans. Geosci. Remote Sens.*, vol. 50, no 5, pp. 1354–1366, May 2012.

[9] D. Entekhabi *et al.*, "The soil moisture active passive (SMAP) mission," *Proc. IEEE*, vol. 98, no 5, pp. 704–716, May 2010.

[10] H. Kim *et al.*, "Global-scale assessment and combination of SMAP with ASCAT (active) and AMSR2 (passive) soil moisture products," *Remote Sens. Environ.*, vol. 204, pp. 260–275, 2018.

[11] H. Ma, J. Zeng, N. Chena, X. Zhang, M. H. Cosh, and W. Wang, "Satellite surface soil moisture from SMAP, SMOS, AMSR2 and ESA CCI: A comprehensive assessment using global ground-based observations," *Remote Sens. Environ.*, vol. 231, 2019, Art. no. 111215.

[12] T. J. Colliander *et al.*, "Validation of SMAP surface soil moisture products with corevalidation sites A," *Remote Sens. Environ.*, vol. 191, pp. 215–231, 2017.

[13] W. Wagner, G. Bloeschl, P. Pamaloni, and J. C. Calvet, "Operational readiness of microwave remote sensing of soil moisture for hydrologic applications," *Nordic Hydrol.*, vol. 38, pp. 1–20, 2007.

[14] M. S. Moran, "Soil moisture evaluation using multi-temporal synthetic aperture radar (SAR) in semiarid rangeland," *Agricultural Forest Meteorol.*, vol. 105, no. 1–3, pp. 69–80, Nov. 2000.

[15] B. Molero *et al.*, "SMOS disaggregated soil moisture product at 1 km resolution: Processor overview and first validation results," *Remote Sens. Environ.*, vol. 180, pp. 361–376, 2016.

[16] N. Pierdicca, L. Pulvirenti, and C. Bignami, "Soil moisture estimation over vegetated terrains using multitemporal remote sensing data," *Remote Sens. Environ.*, vol. 114, pp. 440–448, 2010.

[17] S. Bousbih *et al.*, "Potential of Sentinel-1 radar data for the assessment of soil and cereal cover parameters," *Sensors*, vol. 17, 2017, Art. no. 2617.

[18] E. Santi, M. Dabboor, S. Pettinato, and S. Paloscia, "Combining machine learning and compact polarimetry for estimating soil moisture from C-band SAR data," *Remote Sens.*, vol. 11, 2019, Art. no. 2451.

[19] A. Gorrab, M. Zribi, N. Baghdadi, B. Mougenot, and Z. Lili-Chaabane, "Retrieval of both soil moisture and texture using TerraSAR-X images," *Remote Sens.*, vol. 7, pp. 10098–10116, 2015.

[20] H. S. Srivastava, P. Patel, Y. Sharma, and R. R. Navalgund, "Large-area soil moisture estimation using multi-incidence-angle RADARSAT-1 SAR data," *IEEE Trans. Geosci. Remote Sens.*, vol. 47, no. 8, pp. 2528–2535, Aug. 2009.

[21] A. Balenzano, F. Mattia, G. Satalino, and M. W. J. Davidson, "Dense temporal series of C- and L-band SAR data for soil moisture retrieval over agricultural crops," *IEEE J. Sel. Top. Appl. Earth Observ. Remote Sens.*, vol. 4, no. 2, pp. 439–450, Jun. 2011.

[22] C. Ma, X. Li, and M. F. McCabe, "Retrieval of high-resolution soil moisture through combination of Sentinel-1 and Sentinel-2 data," *Remote Sens.*, vol. 12, 2020, Art. no. 2303.

[23] H. Wang, R. Magagi, K. Goïta, and T. Jagdhuber, "Refining a polarimetric decomposition of multi-angular UAVSAR time series of soil moisture retrieval over low and high vegetated agricultural fields," *IEEE J. Sel. Top. Appl. Earth Observ. Remote Sens.*, vol. 12, no. 5, pp. 1431–1450, May 2019.

[24] H. Wang, R. Magagi, K. Goïta, T. Jagdhuber, and I. Hajnsek, "Evaluation of simplified polarimetric decomposition for soil moisture retrieval over vegetated agricultural fields," *Remote Sens.*, vol. 8, 2016, Art. no. 142.

[25] N. E. C. Verhoest, H. Lievens, W. Wagner, J. Alvarez-Mozos, M.S. Moran, and F. Mattia, "On the soil roughness parameterization problem in soil moisture retrieval of bare surfaces from synthetic aperture radar," *Sensors*, vol. 8, pp. 4213–4248, 2008.

[26] A. Balenzano *et al.*, "A ground network for SAR-derived soil moisture product calibration validation and exploitation in southern italy," in *Proc. IEEE Int. Geosci. Remote Sens. Symp.*, 2014, pp. 3382–3385.

[27] M. Zribi *et al.*, "Soil moisture mapping in a semiarid region, based on ASAR/wide swath satellite data," *Water Resour. Res.*, vol. 50, no. 2, pp. 823–835, 2014.

[28] B. Bauer-Marschallinger *et al.*, "Toward global soil moisture monitoring with Sentinel-1: Harnessing assets and overcoming obstacles," *IEEE Trans. Geosci. Remote Sens.*, vol. 57, no. 1, pp. 520–539, Jan. 2019.

[29] M. Foucras, M. Zribi, C. Albergel, N. Baghdadi, J. C. Calvet, and T. Pellarin, "Estimating 500-m resolution soil moisture using Sentinel-1 and optical data synergy," *Water*, vol. 12, 2020, Art. no. 866.

[30] J. Shi, J. Wang, A. Y. Hsu, P. E. O'Neill, and E. T. Engman, "Estimation of bare surface soil moisture and surface roughness parameter using L-band SAR image data," *IEEE Trans. Geosci. Remote Sens.*, vol. 35, no. 5, pp. 1254–1266, Sep. 1997.

[31] S. B. Kim, M. Moghaddam, L. Tsang, M. Burgin, X. Xu, and E. G. Njoku, "Models of L-band radar backscattering coefficients over global terrain for soil moisture retrieval," *IEEE Trans. Geosci. Remote Sens.*, vol. 52, no. 2, pp. 1381–1396, Feb. 2014.

[32] S. B. Kim *et al.*, "Surface soil moisture retrieval using the L-band synthetic aperture radar onboard the soil moisture active–passive satellite and evaluation at core validation sites," *IEEE Trans. Geosci. Remote Sens.*, vol. 55, no. 4, pp. 1897–1914, Apr. 2017.

[33] J. Ezzahar *et al.*, "Evaluation of backscattering models and support vector machine for the retrieval of bare soil moisture from Sentinel-1 data," *Remote Sens.*, vol. 12, no. 1, 2020, Art. no. 72.

[34] C. Notarnicola, M. Angiulli, and F. Posa, "Soil moisture retrieval from remotely sensed data: Neural network approach versus Bayesian method," *IEEE Trans. Geosci. Remote Sens.*, vol. 46, no. 2, pp. 547–557, Feb. 2008.

[35] E. Santi, S. Paloscia, S. Pettinato, and G. Fontanelli, "Application of artificial neural networks for the soil moisture retrieval from active and passive microwave spaceborne sensors," *Int. J. Appl. Earth Observ. Geoinf.*, vol. 48, pp. 61–73, 2016.

[36] M. E. Hajj, N. Baghdadi, M. Zribi, and H. Bazzi, "Synergic use of Sentinel-1 and Sentinel-2 images for operational soil moisture mapping at high spatial resolution over agricultural areas," *Remote Sens.*, vol. 9, 2017, Art. no. 1292.

[37] W. Wagner, G. Lemoine, and H. Rott, "A method for estimating soil moisture from ERS scatterometer and soil data," *Remote Sens. Environ.*, vol. 70, pp. 191–207, 1999.

[38] W. Wagner *et al.*, "Temporal stability of soil moisture and radar backscatter observed by the advanced synthetic aperture radar (ASAR)," *Sensors*, vol. 8, pp. 1174–1197, 2008.

[39] Q. Gao, M. Zribi, M. J. Escorihuela, and N. Baghdadi, "Synergetic use of Sentinel-1 and Sentinel-2 data for soil moisture mapping at 100 m resolution," *Sensors*, vol. 17, 2017, Art. no. 1966.

[40] S. K. Tomer *et al.*, "Retrieval and multi-scale validation of soil moisture from multi-temporal SAR data in a tropical region," *Remote Sens.*, vol. 7, pp. 8128–8153, 2015.

[41] H. Bazzi, N. Baghdadi, M. E. Hajj, M. Zribi, and H. Belhouchette, "A comparison of two soil moisture products S2MP and copernicus-SSM over Southern France," *J. Sel. Top. Appl. Earth Observ. Remote Sens.*, vol. 12, no. 9, pp. 3366–3375, Sep. 2019.

[42] F. T. Ulaby, R. K. Moore, and A. K. Fung, "Physical mechanisms and empirical models for scattering and emission," *Microw. Remote Sens.*, vol. 2, pp. 816–921, 1982.

[43] A. K. Fung, Z. Li, and K. S. Chen, "Backscattering from a randomly rough dielectric surface," *IEEE Trans. Geosci. Remote Sens.*, vol. 30, no. 2, pp. 356–369, Mar. 1992.

[44] A. K. Fung, *Microwave Scattering and Emission Models and Their Applications*. Norwood, MA, USA: Artech House, 1994.

[45] Q. Li, J. C. Shi, and K. S. Chen, "A generalised power law spectrum and its applications to the backscattering of soil surfaces based on the integral equation model," *IEEE Trans. Geosci. Remote Sens.*, vol. 40, no. 2, pp. 271–280, Feb. 2002.

[46] F. Mattia, T. L. Toan, and M. Davidson, "An analytical, numerical, and experimental study of backscattering from multiscale soil surfaces," *Radio Sci.*, vol. 36, no. 1, pp. 119–135, 2001.

[47] M. Baghdadi and M. Zribi, "Characterization of soil surface properties using radar remote sensing," in *Proc. Land Surf. Remote Sens. Continental Hydrol.*, 2016, pp. 1–39.

[48] B. Cappelaere *et al.*, "The AMMA-CATCH experiment in the cultivated sahelian area of south-west Niger - Investigating water cycle response to a fluctuating climate and changing environment," *J. Hydrol.*, vol. 375, pp. 34–51, 2009.

[49] C. Velluet *et al.*, "Building a field-and model-based climatology of local water and energy cycles in the cultivated Sahel-Annual budgets and seasonality," *Hydrol. Earth Syst. Sci.*, vol. 18, no. 12, pp. 5001–5024, 2014.

[50] C. Calvet, N. Fritz, F. Froissard, D. Suquia, A. Petitpa, and B. Piguet, "In situ soil moisture observations for the CAL/VAL of SMOS: The SMOSMANIA network," in *Proc. IEEE Int. Geosci. Remote Sens. Symp.*, 2007, pp. 1196–1199.

[51] M. Schwerdt *et al.*, "Independent system calibration of Sentinel-1B," *Remote Sens.*, vol. 9, 2017, Art. no. 511.

[52] M. Zribi and M. Dechambre, "An new empirical model to retrieve soil moisture and roughness from radar data," *Remote Sens. Environ.*, vol. 84, no. 1, pp. 42–52, 2003.

[53] J. Zeng, K. S. Chen, H. Bi, Q. Chen, and X. Yang, "Radar response of off-specular bistatic scattering to soil moisture and surface roughness at L-band," *IEEE Geosci. Remote Sens. Lett.*, vol. 12, no. 13, pp. 1945–1949, Dec. 2016.
[54] M. T. Hallikanen, F. T. Ulaby, M. C. Dobson, M. El-Rayes, and L. Wu, "Microwave dielectric behavior of wet Soil- Part I: Empirical models and experimental observations," *IEEE Trans. Geosci. Remote Sens.*, vol. GE-23, no. 1, pp. 25–34, Jan. 1985.
[55] F. T. Ulaby, R. K. Moore, and A. K. Fung, *Microwave Remote Sensing Active and Passive*. Norwood, MA, USA: Artech House, 1986.
[56] M. E. Hajj, N. Baghdadi, B. Cheviron, M. Zribi, and S. Angelliaume, "Analysis of Sentinel-1 radiometric stability and quality for land surface applications," *Remote Sens.*, vol. 8, no. 5, 2016, Art. no. 406.
[57] T. Pellarin, J. C. Calvet, and W. Wagner, "Evaluation of ERS scatterometer soil moisture products over a half-degree region in southwestern France," *Geophys. Res. Lett.*, vol. 33, no. 17, pp. 1–6, Sep. 2006, doi: 10.1029/2006GL027231.
[58] Y. Pachepsky and W. J. Rawls, *Development of Pedotransfer Functions in Soil Hydrology*. New York, NY, USA: Elsevier, 2004.
[59] M. Zribi, A. Gorrab, N. Baghdadi, and Z. Lili-Chabaane, "Influence of radar frequency on the relationship between bare surface soil moisture vertical profile and radar backscatter," *IEEE Geosci. Remote Sens. Lett.*, vol. 11, no. 4, pp. 848–852, Apr. 2014.

Mehrez Zribi received the B.E. degree in signal processing from the Ecole Nationale Supérieure d'Ingénieurs en Constructions Aéronautiques, Toulouse, France, in 1995, and the Ph.D. degree in remote sensing from the Université Paul Sabatier, Toulouse, France, in 1998.

He is a Research Director with the Centre National de Recherche Scientifique. In 1995, he was with the Centre d'Etude des Environnements Terrestre et Planétaires Laboratory/Institut Pierre Simon Laplace, Vélizy, France. Since October 2008, he has been with the Centre d'Etudes Spatiales de la Biosphère, Toulouse. He has authored/coauthored more than 130 articles in refereed journals. He is currently deputy director of CESBIO. His research interests include microwave remote sensing applied to hydrology, microwave modeling for land surface parameters estimations, and finally airborne microwave instrumentation.

Myriam Foucras received the master's degree in applies mathematics from the University of Paul Sabatier, Toulouse, France, in 2010, and the Ph.D. degree in telecommunications from ENAC (French School of Civil Aviation), Toulouse, France, in 2015.

She worked with the spatial industry for several years on Galileo program. Since 2018, she has been a Research Engineer with CESBIO. Her research interests include GNSS signal processing and reflectometry for land surface applications.

Nicolas Baghdadi received the Ph.D. degree in remote sensing from the University of Toulon, Toulon, France, in 1994.

From 1995 to 1997, he was a Postdoctoral Researcher with INRS Ete—Water Earth Environment Research Centre, Quebec University, QC, Canada. From 1998 to 2008, he was with the French Geological Survey (BRGM), Orléans, France. Since 2008, he has been a Senior Scientist with the National Research Institute for Agriculture, Food and the Environment, Montpellier, France. He is the Editor of two series of books "*Land Surface Remote Sensing Set*" and "*QGIS in Remote Sensing Set*" (http://www.iste.co.uk/subject.php?id = NJNK). His research interests include microwave remote sensing, image processing, satellite and airborne remote sensing data analysis, remote sensing data (SAR, Lidar, optical), and the retrieval of environmental parameters (e.g., soil moisture content, surface roughness, biomass).

Dr. Baghdadi is currently the Scientific Director of the THEIA Land Data Centre (https://www.theia-land.fr/en).

Jerome Demarty received the Ph.D. degree in hydrology from the Paris Diderot University, Paris, France, in 2001.

He has been working for 12 years as Researcher with the HydroSciences Montpellier Laboratory, French Institute of Research for the development, France. His research interests include ecohydrology, surface modeling, and remote sensing, especially on Sahelian and Mediterranean ecosystems.

Sekhar Muddu received the Ph.D. degree in hydrology & water resources from the Indian Institute of Science, Bangalore, India, in 1993.

Since 1994, he has been with the Department of Civil Engineering, Indian Institute of Science, and he is currently a Professor.

Prof. Muddu is also a member of the scientific team with the Indo-French Cell for Water Sciences, IISc. He is collaborating with interdisciplinary teams on integrated hydrological and geochemical catchment experiments and is a Leading Member of the Kabini CZO and AMBHAS Observatory. His research interests include analysis, modeling and process understanding of groundwater systems, and satellite hydrology.